Electronic Supplementary information for

Laser-Engineered Oxygen Vacancies for Improving NO_2 Sensing Performance of SnO_2 Nanowires

Yong Jung Kwon,[a†] Hyoun Woo Kim,[b†] Woo Chul Ko,[a] Heechae Choi[c] , Yong-Ho Ko[d], and Young Kyu Jeong[a,*]

[a.1] *Non-Ferrous Materials Group, Korea Institute of Industrial Technology (KITECH), 137-41 Gwahakdanji-ro, Gangneung-si, Gangwon 25440, Republic of Korea*
[b.2] *Division of Materials Science and Engineering, Hanyang University, Seoul 133-791, Republic of Korea*
[c.3] *Theoretical Materials & Chemistry Group, Institute of Inorganic Chemistry, University of Cologne, Greinstr. 6, 50939, Cologne, Germany*
[d.] *Joining R&D Group/Micro-joining Center, Korea Institute of Industrial Technology (KITECH), 156, Gaetbeol-ro, Yeonsu-gu, Incheon, 21999, Republic of Korea*
** Corresponding author: immrc80@gmail.com*

Figure S1

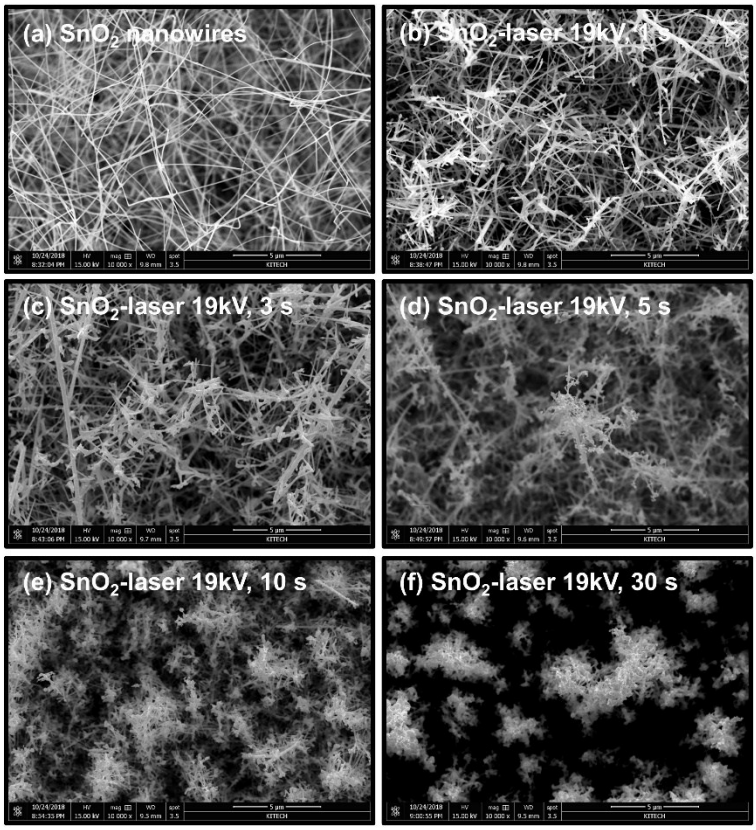

Figure S1. Low magnification SEM images of (a) pristine SnO_2 nanowires and (b-f) SnO_2 nanowires irradiated by laser for (b) 1, (c) 3, (d) 5, (e) 10, and (f) 30 s.

Low magnification SEM images shown in Figure S1 confirm that the longer the laser irradiation time, the smaller the surface area of the sensing materials.

Figure S2

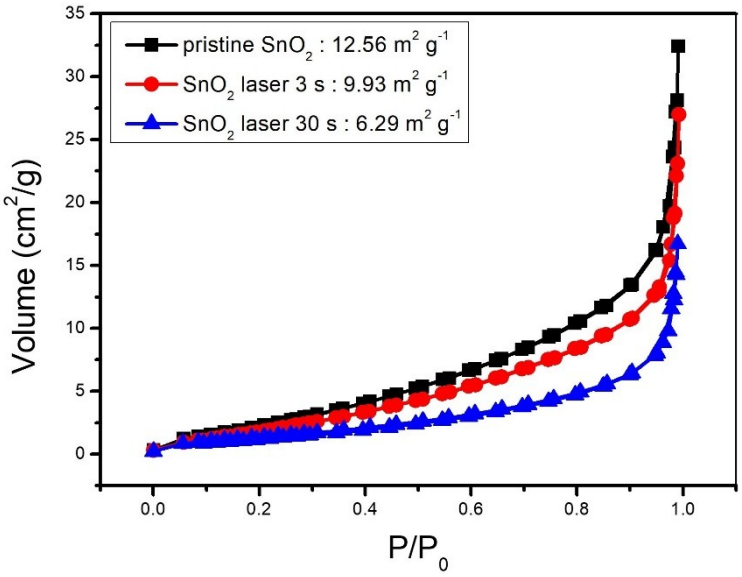

Figure S2. Typical nitrogen adsorption-desorption isotherms of the pristine SnO_2 nanowires and SnO_2 nanowires irradiated by laser for 3 and 30 seconds. The BET surface areas of pristine SnO_2 nanowires and SnO_2 nanowires irradiated by laser for 3 and 30 s is 12.56, 9.93 and 6.29 $m^2 \cdot g^{-1}$, respectively.

Nitrogen (N_2) adsorption–desorption isotherms at 77K were measured on BELSORP-mini II instrument (BEL Japan, Inc.), and the specific surface areas were calculated using the Brunauer-Emmett-Teller (BET) method.[1] For accuracy of data, about 50 mg of powder for each sample was scraped from the substrate using a sharp blade. The powders were placed into cells and pretreated overnight for degas at 250 °C before determining the mass of the material. Typical adsorption-desorption isotherms for the pristine SnO_2 nanowires and SnO_2 nanowires irradiated by laser for 3 and 30 s are shown in figure S2. The BET surface area of the pristine SnO_2 nanowires and SnO_2 nanowires irradiated by laser for 3 and 30 s is 12.56, 9.93 and 6.26 $m^2 g^{-1}$, respectively. The reduction in the specific surface area with increasing laser irradiation time can be explained with the laser-induced thermal aggregation of molten nanowires that involves with the laser ablation process. Considering that the large surface to volume ratio is highly desired for fabricating high performance gas sensing materials, the observed BET result clearly supports our claim that the improved sensing performance in laser irradiated samples predominantly arises from the formation of oxygen vacancy defects.

Figure S3

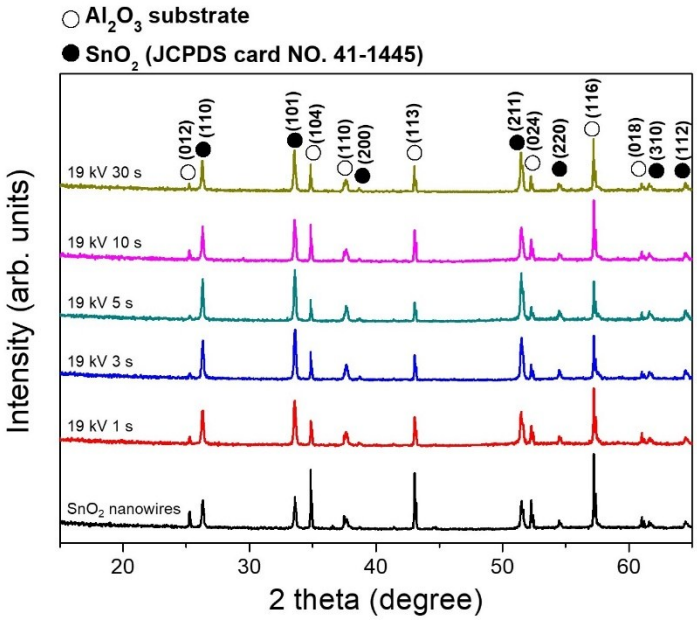

Figure S3. XRD spectra of pristine SnO_2 nanowires and SnO_2 nanowires irradiated by laser for 1, 3, 5, 10, and 30s.

Figure S3 shows the typical XRD patterns of the non-irradiated SnO_2 nanowires and the irradiated SnO_2 nanowires with different irradiation times of 1, 3, 5, 10, and 30 s. The patterns show reflection peaks that can be indexed to a tetragonal rutile SnO_2 phase (JCPDS card: No. 41-1445). The pulsed laser irradiation does not significantly contribute to the formation of other phases such as tin monoxides.

Figure S4

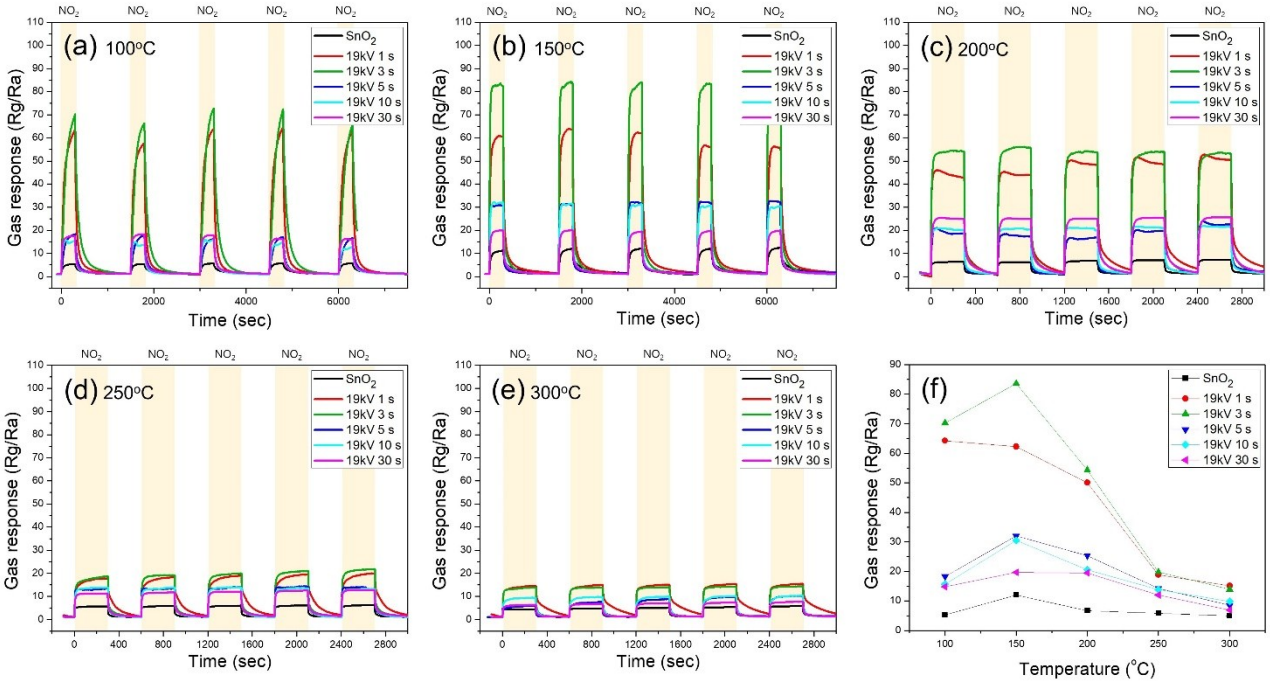

Figure S4. The NO_2 response curves of the pristine SnO_2 and laser irradiated SnO_2 sensors at (a) 100, (b) 150, (c) 200, (d) 250 and (e) 300 °C. (f) Variation of the NO_2 response as a function of working temperature ranging from 100−300 °C for the pristine SnO_2 and laser irradiated SnO_2.

Figure S4(a)-(e) show dynamic response curves toward NO_2 gas for the pristine and laser-irradiated SnO_2 sensors at 100, 150, 200, 250, 300 °C, respectively, and these results are summarized in Figure S4(f). All laser-irradiated samples exhibited stronger NO_2 responses than the pristine SnO_2 nanowires at all working temperatures. Among them, in particular, the one irradiated for 3 seconds presented the best performance; it demonstrated remarkable enhancement with maximum responses of 70.23 and 83.62 at 100 °C and 150 °C, respectively, which are 14 and 7 times higher than that of the pristine SnO_2 sample, suggesting that the optimal working temperature is 100 °C. Also, note that all sensors showed a bell-shaped response behavior; the response initially increased, reached a maximum at 100-150° C, and then decreased as the working temperature increased beyond 150 °C, which is a typical feature in semiconductor gas sensors.

Figure S5

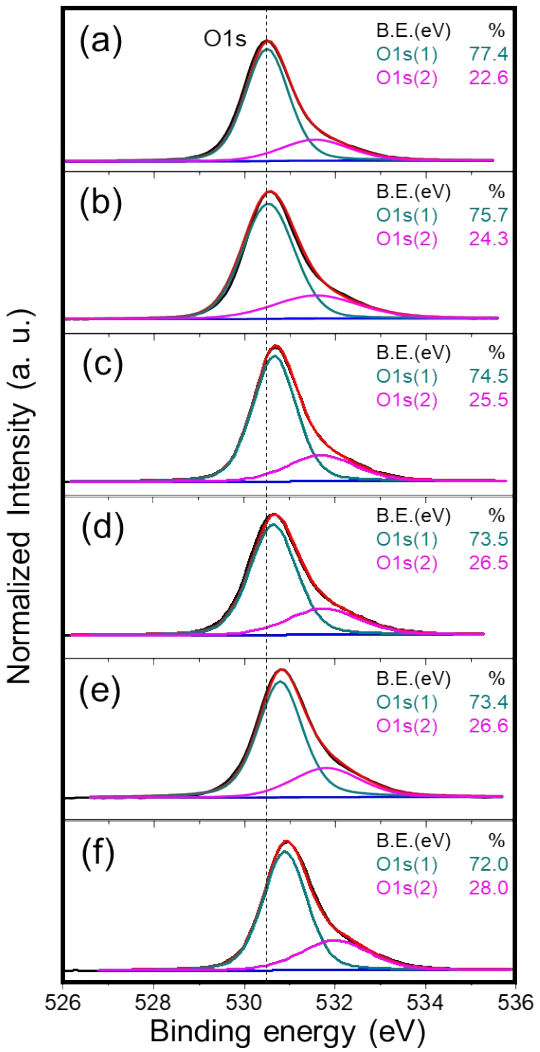

Figure S5. XPS O1s spectra of the (a) pristine SnO_2 nanowires and (b-f) SnO_2 nanowires irradiated by laser for (b) 1, (c) 3, (d) 5, (e) 10, and (f) 30 s

The XPS O1s spectra of the (a) pristine SnO_2 nanowires and (b-f) SnO_2 nanowires irradiated with laser for (b) 1, (c) 3, (d)5, (e) 10, and (f) 30 s are shown in the Figure S5. The all spectra in O 1s core levels have a wide and asymmetric XPS spectrum, which is fitted with two peaks located at 530.4 and 531.6 eV, respectively. The high intense peak [O1s(1)] can be assigned to the O 1s core level of the oxygen anions bounded to Sn^{4+} ion, and the shoulder peak [O1s(2)] is proposed to be nonstoichiometries and disorder stemming from surface oxygen vacancies.[2,3] The relative concentration of the O1s(2) peak is found to increase as the irradiation time increases, supporting that the laser irradiation promotes the formation of oxygen vacancies.

Figure S6

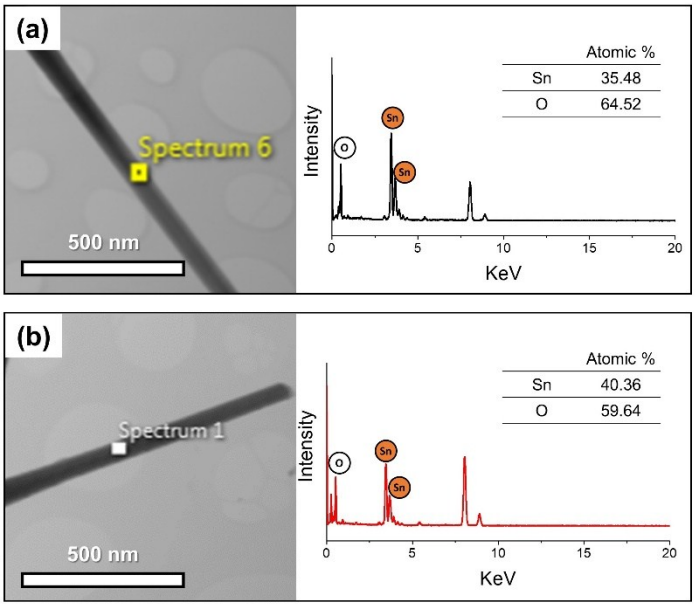

Figure S6. Typical TEM image and corresponding EDS patterns of (a) pristine SnO_2 nanowires and (b) SnO_2 nanowires irradiated by laser for 3 s.

.

Figure S6 presents the EDS data, which were measured based on the TEM analysis. In the pristine SnO_2 nanowire, the atomic concentration ratios of Sn and O were estimated to be approximately 38.7% and 61.3%, respectively. After irradiation for 3 s, the atomic concentration ratios of Sn and O changed to 41.3% and 58.7%, respectively. It is noteworthy that the oxygen atomic ratio decreased from 61.3% to 58.7% upon irradiation, whereas the Sn atomic ratio increased from 38.7% to 41.3%. The O atomic ratio decreased by 2.6% in the TEM-EDS analysis. Based on the EDS analysis, we surmise that the oxygen atoms would be released from the SnO_2 lattice, forming oxygen vacancies.

Figure S7

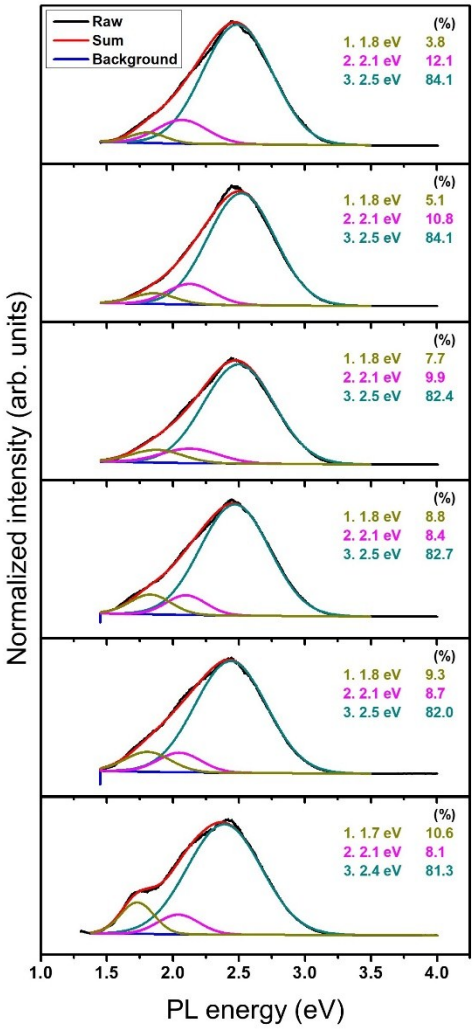

Figure S7. PL spectra of (a) pristine SnO_2 nanowires and SnO_2 nanowires irradiated by laser for (b) 1, (c) 3, (d) 5, (e) 10, and (f) 30 s.

We performed photoluminescence (PL) analysis to investigate the effects of pulsed laser irradiation on the surface chemical states of the laser-treated SnO_2 nanowire and its relation to the sensing behavior of SnO_2. In Figure S3, we present the PL spectra of the non-irradiated and irradiated SnO_2 nanowires. The irradiation time was set to 1, 3, 5, 10, and 30 s. The PL spectra were deconvoluted into three Gaussian peaks, corresponding to the peaks at 1.9 (1.85~1.95), 2.1 (2.0~2.2), and 2.5 (2.4~2.6) eV. There are two types of SnO_2 crystal oxygen vacancies, namely, bridging oxygen (O^B) and in-plain oxygen (O^P) vacancies.[4] Yellow and blue-green luminescence are attributed to the O^B vacancies and O^P vacancies, respectively.[5–7] The 1.9-eV emission

originates from the O^B vacancies.[8] The 2.1-eV emission originates from the structural defects or tin interstitials.[9] The 2.5-eV emission is associated with the O^P vacancies (singly charged oxygen vacancy).[10] It is noteworthy that the relative intensity of the peak at 1.9 eV with regard to the other peaks at 2.1 and 2.5 eV is enhanced by means of the pulsed laser irradiation. Furthermore, the relative intensity of the peak at 1.9 eV with regard to the peaks at 2.1 and 2.5 eV increases with increasing irradiation time in the range of 1–30 s. These results demonstrate not only the formation of O^B vacancies in the SnO_2 structure by laser irradiation but also the increase in the amount of O^B vacancies by increasing the irradiation time.

TEXT S1. Vacancy reaction equation

When the n-type SnO_2 sensors are irradiated with laser, the oxygen vacancies are formed on the SnO_2 surfaces, simultaneously generating two free electrons according to the reaction equation (1).[11]

$$O_o \rightarrow Vo^{2+} + 2\ e^- + 1/2O_{2(gas)} \quad (1)$$

Then, when the sensors are exposed to air, the oxygen molecules (O_2) adsorb on the SnO_2 surfaces by capturing these electrons to form negatively charged ions such as O_2^-, O^{2-}, O^- [reactions (3), (4) and (5)].

$$O_{2(ads)} + e^- \rightarrow O_2^-{}_{(ads)} \quad (3)$$

$$O_2^-{}_{(ads)} + e^- \rightarrow 2O^-{}_{(ads)} \quad (4)$$

$$O^-{}_{(ads)} + e^- \rightarrow O^{2-}{}_{(ads)} \quad (5)$$

When the SnO_2 sensors are exposed to the NO_2 target gas, they further release the free electrons to the adsorbed NO_2 molecules, making them more electron deficient [reaction (6)].[12] In this way, the conduction channels of SnO_2 can be modulated resulting in variation in sensor resistance.

$$NO_{2(gas)} + 2e^- \rightarrow NO^{2-}{}_{(ads)} \quad (6)$$

References in Electronic Supplementary information

1 K. S. W. Sing, D. H. Everett, R. A. W. Haul, L. Moscou, R. A. Pierotti, J. Rouquerol and T. Siemieniewska, *Pure Appl. Chem.*, 1985, **57**, 603–619.

2 C. Wang, G. Du, K. Stahl, H. Huang, Y. Zhong and J. Z. Jiang, *J. Phys. Chem. C*, 2012, **116**, 4000–4011.

3 V. Kumar, V. Kumar, S. Som, J. H. Neethling, M. Lee, O. M. Ntwaeaborwa and H. C. Swart, *Nanotechnology*, 2014, **25**, 135701.

4 V. Bonu, A. Das, S. Amirthapandian, S. Dhara and A. K. Tyagi, *Phys. Chem. Chem. Phys.*, 2015, **17**, 9794-9801.

5 V. Bonu, A. Das, A. K. Prasad, N. G. Krishna, S. Dhara and A. K. Tyagi, *Appl. Phys. Lett.*, 2014, **105**, 243102.

6 S. Lettieri, M. Causà, A. Setaro, F. Trani, V. Barone, D. Ninno and P. Maddalena, *J. Chem. Phys.*, 2008, **129**, 244710.

7 J. D. Prades, J. Arbiol, A. Cirera, J. R. Morante, M. Avella, L. Zanotti, E. Comini, G. Faglia and G. Sberveglieri, *Sens. Actuators B Chem.*, 2007, **126**, 6-12.

8 V. A. Gercher, D. F. Cox, *Surf. Sci.*, 1995, **322**, 177-184.

9 S. Shi, D. Gao, Q. Xu, Z. Yang and D. Xue, *RSC Adv.,* 2014, **4**, 45467-45472

10 J. Jeong, S.-P. Choi, C. I. Chang, D. C. Shin, J. S. park, B.-T. Lee, Y.-J. Park and H.-J. Song, *Solid State Commun.,* 2003, **127**, 595-597.

11 S. S. Kim, H. G. Na, H. W. Kim, V. Kulish and P. Wu, *Sci. Rep.*, 2015, **5**, 10723.

12 S. Kannan, H. Steinebach, L. Rieth and F. Solzbacher, *Sens. Actuatators B Chem.*, 2010, **148**, 126–134.